Int J Biometeorol (2011) 55:435–446
DOI 10.1007/s00484-010-0354-9

ORIGINAL PAPER

Climate-based models for West Nile *Culex* mosquito vectors in the Northeastern US

Hongfei Gong · Arthur T. DeGaetano · Laura C. Harrington

Received: 4 February 2010 / Revised: 22 July 2010 / Accepted: 30 July 2010 / Published online: 5 September 2010

Abstract Climate-based models simulating *Culex* mosquito population abundance in the Northeastern US were developed. Two West Nile vector species, *Culex pipiens* and *Culex restuans*, were included in model simulations. The model was optimized by a parameter-space search within biological bounds. Mosquito population dynamics were driven by major environmental factors including temperature, rainfall, evaporation rate and photoperiod. The results show a strong correlation between the timing of early population increases (as early warning of West Nile virus risk) and decreases in late summer. Simulated abundance was highly correlated with actual mosquito capture in New Jersey light traps and validated with field data. This climate-based model simulates the population dynamics of both the adult and immature mosquito life stage of *Culex* arbovirus vectors in the Northeastern US. It is expected to have direct and practical application for mosquito control and West Nile prevention programs.

Keywords Climate-based · Population model · West Nile virus · *Culex pipiens* · *Culex restuans* · Mosquito · Vector-borne disease control

H. Gong · L. C. Harrington
Entomology Department, Cornell University,
Ithaca, NY 14853, USA

A. T. DeGaetano (✉)
Earth and Atmospheric Science Department, Cornell University,
Ithaca, NY 14853, USA
e-mail: atd2@cornell.edu

Introduction

Although daily weather and seasonal to inter-annual climatic variability influence mosquito vector biology and risk of vector-borne disease, this information is not readily employed in disease control programs. Rather, such programs rely typically on trap-based surveillance (e.g., Reisen et al. 1999; White 2006; Krockel et al. 2006). Although traps provide a cost-effective means of establishing relative mosquito abundance, the resulting count data are highly variable in space and affected by non-biological day-to-day changes in trapping efficiency. Because of this, long-term historical count records provide useful benchmarks only if trap locations (and the environment adjacent to static trap locations) remain constant through the record. Similarly, count data alone provide little insight into potential changes in relative mosquito abundance under altered climate conditions.

From a practical standpoint, the collection and identification of trap data is time-intensive, diminishing the utility of data in operational control and public health advisories. This is further complicated by the fact that the traps provide only a snapshot of relative mosquito abundance at specific locations, rather than a broader (e.g., county-scale) measure of mosquito prevalence. This disconnect in spatial scale is one possible reason why climatic information is not used routinely as a part of vector management or public health awareness strategies. Although related, the local scale environmental factors that drive catch at a particular trap are often not reflective of the broader regional climate conditions that influence relative mosquito abundance over a wider area.

Several models have been developed to describe population dynamics of mosquito disease vectors using

climate data. Some, but not all, models include the effect of temperature, which drives mosquito development, and rainfall, which provides availability of breeding sites for mosquitoes. However, rainfall may also reduce larval survival through flushing effects (Koenraadt and Harrington 2008) and can reduce trap counts (DeGaetano 2005) used for estimating mosquito populations. Several detailed studies have been developed for specific vectors. For example, Focks et al. (1993a) developed a detailed model to describe the life history of the dengue and yellow fever vector, *Aedes aegypti*. Ahumada et al. (2004) developed a matrix model based on temperature and rainfall for the avian malaria vector in Hawaii, *Culex quinquefasciatus*, and successfully simulated field results. Shone et al. (2006) were able to describe populations of the saltmarsh mosquito *Aedes sollicitans* in Maryland using time-dependent Poisson regression models. Unfortunately, however, many models describing vector population dynamics contain assumptions about the basic biology and ecology of mosquitoes that are difficult to validate in field settings.

Furthermore, a significant number of models for vector-borne infections do not take into account the variation in vector population dynamics that is a key driver of transmission (Esteva and Vargas 1999; Derouich et al. 2003; Ngwa 2004). Despite the value of models for conceptualizing the relative role of different parameters in the vector-borne disease cycle, few models have been developed that are employed on a regular basis in vector-borne disease surveillance activities (Focks et al. 1993a, b, 1995; Eisenberg et al. 1995; Ahumada et al. 2004). Wonham et al. (2004) describe an epidemiological model for West Nile virus (WNV) with direct applicability to mosquito control.

Given that abiotic and environmental factors can vary greatly at small geographical scales, developing models that are adaptable to different environments is critical. In addition, there are large gaps in the understanding of how climate and environmental change influence mosquito vectors and ultimately vector-borne disease transmission. There is a critical need to fill knowledge gaps for these systems, both in the United States (Ebi et al. 2006) and globally.

As a first step towards improving knowledge of climate and vector-borne disease patterns, two models to simulate the activity of *Culex pipiens and Culex restuans* arbovirus vectors in the Northeastern US were developed and tuned with laboratory and field data. WNV has become an endemic infection in the US since its introduction in the New York metropolitan area (CDC 1999a, b). WNV introduction, and now endemic transmission, in the US provide an opportunity to develop models that will be useful and adaptable to other existing arboviruses and future introductions of novel mosquito-borne pathogens into the region.

The goals of this study were (1) to understand how climate and environment affect mosquito populations at the microhabitat level; (2) to develop methods to scale data from the microhabitat level to a broader (several square kilometer) area using regional weather observations; and (3) to develop a prototype for a reliable predictive model that can be adapted for mosquito control and public health professionals in a variety of settings. Ultimately, the incorporation of a pathogen component to the model is planned. The initial focus was two *Culex* species (*Cx. pipiens* and *Cx. restuans*) that may be important in local transmission of vector-borne diseases that involve avian amplification cycles. Long-term data sets of adult abundance were utilized, and larval development with temperature and precipitation in local habitats was investigated by sampling, identifying and staging larvae with return to the field habitats.

Materials and methods

Mosquito collection data

Historical mosquito collection data were available for model development from New Jersey Light trap collections from mosquito abatement districts with the following locations and years: Site 1, North Brunswick, Middlesex County, New Jersey (40.4°N,74.5°W) 1990–1993, 1997, 1999, 2001 and Site 2, near Cambridge, Dorchester County, Maryland (38.56°N, 76.07°W) 1975,1977,1982–1985. A New Jersey Light trap at site 1 was operated from 1984 to 2004, and at site 2 from 1958 to 1989. At site 1, 1990–2001 data and at site 2, 1974–1977 and 1980–1986 data were used for this study based on the completeness of data in individual years. Traps were run from dusk to dawn Monday–Friday from 1 June to 15 September.

These data highlight the spatial variations in trap catch that may occur across a county-size area. In Fig. 1, 7-day running mean trap counts from the North Brunswick site are plotted with coincident data from two other traps within Middlesex County. The Carteret trap is located approximately 32 km to the northeast of the North Brunswick trap. The Edison trap is at an intermediate location, approximately 13 km to the northeast of the North Brunswick trap. Using 1993 as a representative example, the between-trap correlation is low, ranging from about 0.55 for Carteret and the other two sites to only about 0.33 for North Brunswick and Edison. Nonetheless, together the three traps reflect the general county-wide trends in mosquito abundance, such as the rapid increase in catch in late May, a broad early-summer peak in capture, and a prolonged mid- to late-summer period of relatively low capture. In addition, finer temporal scale features such as secondary count peaks

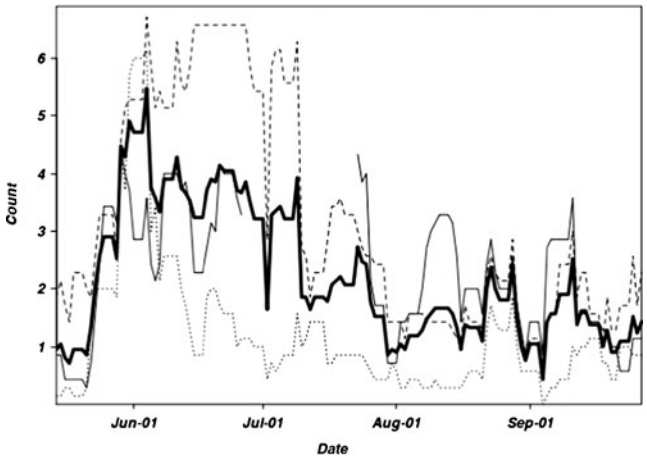

Fig. 1 Comparison of *Culex* capture at three trapping locations in Middlesex County, New Jersey (NJ): *thin solid line* North Brunswick, *dashed line* Carteret, *dotted line* Edison. The average capture across the three traps is given by the *heavy solid line*

around 15 June and mid-September, and local count minima in early June and later in September are well represented by all traps.

In addition, side-by-side NJ light trap and Centers for Disease Control (CDC) trap collections were conducted at a local field site to further validate model simulations in an independent geographical location and relate data from the two types of surveillance traps. The site was located at a farm in Freeville, New York (42° 31′ 52″ N, 76° 19′ 41″ W). Traps were operated on alternate days with collections from the light traps made on Tuesday and Thursday, and the CDC collections made on Wednesday and Friday. Figure 2 shows the total weekly counts from these traps. Like Site 1, the side-by-side trap counts are not strongly correlated (r=0.41, omitting the first week, which is uncharacteristically low for the CDC trap). However, the general seasonal pattern of mid-July and mid-August peaks and a sharp late-August (early-September) decline is reflected by both traps, albeit with a lag of as much as a week.

Mosquitoes collected in traps were identified to genus and, in some cases, to species by mosquito abatement district personnel for historical data sets. Routinely, *Culex* species were not differentiated, necessitating the grouping of species, because it can be difficult to reliably identify and differentiate *Cx. pipiens* and *Cx. restuans* adults (Harrington and Poulson 2008). The counts of grouped species are typically used in operational mosquito control and surveillance programs, with the prevalence of *Cx. pipiens* relative to *Cx. restuans* influenced to some extent by degree day accumulation (Kunkel et al. 2006). For sites 1 and 2, overall *Culex* counts represented *Culex pipiens, Cx. restuans* and *Culex salinarius*. Mosquitoes in more recent collections from New York State were identified to species as larvae and to genus as adults in our laboratory using standard published keys (Means 1987; Andreadis et al. 2005). Total *Culex* capture for historical data sets were averaged over a 7-day period (3 days prior and 3 days after and including current day) to smooth abundance parameters and account for daily sampling inconsistencies.

Meteorological and local scale environmental data

Daily average temperature, rainfall and evaporation near each trap location were obtained from the National Oceanic and Atmospheric Administration (NOAA) Northeast Regional Climate Center. In addition, hourly air temperature at the New York collection site was gathered at the microhabitat level using HOBO data loggers (Onset® Computer Corporation, Bourne, MA). Hourly daylight was computed for each location using standard astronomical equations (e.g., Walraven 1978).

Model development and structure

The models were developed to encompass both immature and adult stages of mosquitoes by separating the life cycle into two distinct stages: immatures (eggs–pupal eclosion) and adults (both males and females from eclosion to death) as shown in Fig. 3.

Two discrete models were developed to simulate the temporal dynamics of *Culex* mosquito populations. Both models used a temperature-dependent function to estimate mosquito development and survival. The degree day (DD) model used the accumulated thermal units above the zero development threshold for *Culex* (see explanation below) to determine the days from egg to adult, while the development rate model used a temperature-dependent function to estimate the percentage of immature mosquitoes to eclose

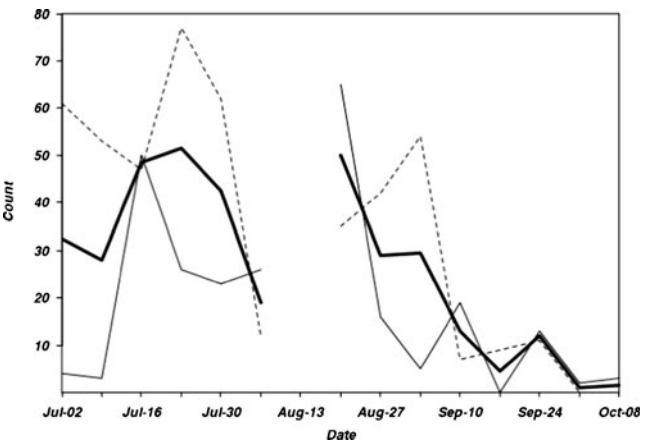

Fig. 2 Total weekly capture during 2006 at co-located Centers for Disease Control (CDC) (*thin solid line*) and NJ light (*dashed line*) traps. The *heavy solid line* shows the average capture. Mechanical problems affected both traps in early August

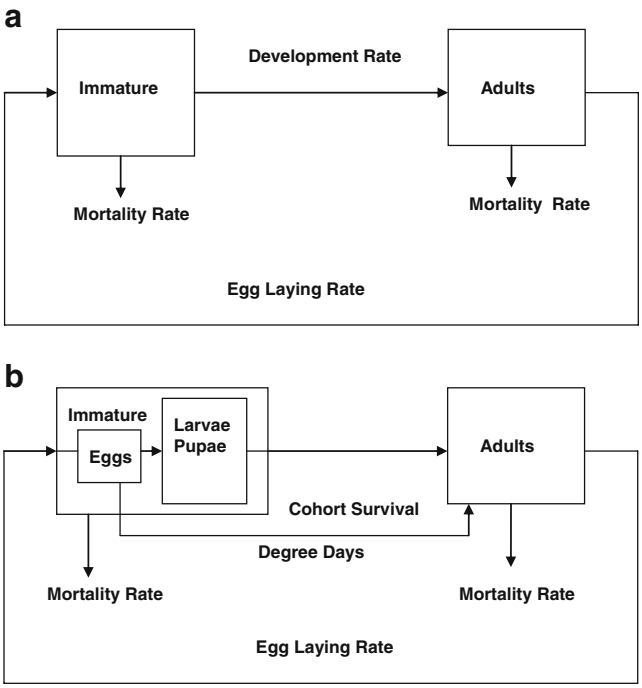

Fig. 3 Schematic diagrams showing variables and the relationship between variables of **a** development rate and **b** degree day (DD) models

on each day. Both models used the functions of "Survival Rate" and "Egg Laying Rate" described below. The following difference equations were used to calculate the population numbers of mosquito immature life stages and adults on each day.

1. Degree day (DD) model

$$N_I(t) = N_I(t-1)^*\delta_I(t-1) + N_A(t-1)^*\beta(t-1) - N_E(t-t_{DD})^*\delta_{EA}(t-t_{DD}) \quad (1)$$

$$N_A(t) = N_A(t-1)^*\delta_A(t-1) + N_E(t-t_{DD})^*\delta_{EA}(t-t_{DD})^*[1-F_d(t-1)] \quad (2)$$

$$N_E(t-t_{DD}) = \beta(t-t_{DD})^*N_A(t-t_{DD}) \quad (3)$$

2. Development rate model

$$N_I(t) = N_I(t-1)^*\delta_I(t-1) + N_A(t-1)^*\beta(t-1) - N_I(t-1)^*\rho_{Dev}(t-1) \quad (4)$$

$$N_A(t) = N_A(t-1)^*\delta_A(t-1) + N_I(t-1)^*\rho_{Dev}(t-1)^*[1-F_d(t-1)] \quad (5)$$

Where (for both models):

N_I	Number of immatures
N_A	Number of adults
N_E	Number of eggs laid
δ_I	Survival rate of immatures
δ_A	Survival rate of adults
δ_{EA}	Survival rate from egg to adults
β	Egg laying rate
ρ_{Dev}	Development rate
F_d	Diapausing fraction of the newly emerged adults
t	Time (days)
t_{DD}	Time (days) to accumulate required number of DD.

All rates are daily and per capita. The survival rates used in the above equations are related to the mortality rates depicted in Fig. 3 by the equation δ=1−mortality rate.

The simulation was started on 1 April and ended on 31 October for each year over the 7-year period at site 1 and the 6-year period at site 2. The mosquito population was initialized every 1 April with a minimum number of 100 eggs and 10 adults.

Functions and parameters

Development rate

Temperature has a major effect on insect development; consequently, the thermal requirements of development are often used as a basis for predicting population dynamics (Wagner et al. 1991). Development rates, ρ_{Dev}, for local strains of *Cx. pipiens* and *Cx. rest*uans were measured in the laboratory under different constant temperatures (10, 15, 20, 25, 30, 32 and 34°C) (Tables 1, 2). In this model, the reciprocal of development time determined from the laboratory was applied as a rate (Wagner et al. 1991). Different functions that have been used to fit development rate results for insects were evaluated and the Sharpe & DeMichele equation (Eq. 6) with four parameters (A, HA, HH, TH) provided the best fit (Fig. 4) [see Rueda et al. (1990) for details].

$$\rho_{Dev} = A^*\frac{K}{298.15}*\frac{\exp\left[\frac{HA}{1.987}*\left(\frac{1}{298.15}-\frac{1}{K}\right)\right]}{1+\exp\left[\frac{HH}{1.987}*\left(\frac{1}{TH}-\frac{1}{K}\right)\right]} \quad (6)$$

Based on the laboratory data A=0.25; HA=28094; HH=35362 and TH=298.60 and, K is the air temperature in units of Kelvin. Equation 6 was applied directly (without further fitting) in the population model.

Degree day conversions

Degree day criteria for mosquito development from egg to adult was determined based on development results from

Table 1 Development time and rate of the New York strain *Culex pipiens* females from egg hatch to adult eclosion

Temperature (°C)	Development time (days)±SEM	Development rate (1/dev. time)
10	52.2±1.4	0.02
15	26.7±1.3	0.04
20	14.6±0.4	0.07
25	8.0±0.1	0.12
30	6.2±0.1	0.16
34	5.6[a]	0.18

[a] Only 1 female survived to adulthood at this temperature

laboratory studies with *Cx. pipiens* (Table 1) and *Cx. restuans* (Table 2). Based on these studies, a basic minimum development threshold of 10°C was identified. Degree day development time was determined by taking the summation of the difference between the hourly temperature and 10°C threshold divided by 24 (Gerade et al. 2004). *Cx. pipiens* and *Cx. restuans* exhibit distinctly different seasonality where they co-occur in North America (Kunkel et al. 2006). Seven years of larval surveillance indicates that *Cx. restuans* is generally abundant in Central New York State from June to July while *Cx. pipiens* is generally abundant from July to August (L. Harrington et al., unpublished data). In our study, the estimate of DD development time for the earlier species, *Cx. restuans*, provided better model performance for both species.

Survival rate

Daily survival rate was estimated using Eq. 7.

$$\delta(t) = S_{op} * \exp\left[-\frac{T(t) - T_{op}}{Var_{Sur}}\right]^2 \quad (7)$$

Where:

$T(t)$ Average daily temperature

Table 2 Development time and rate of the New York strain *Culex restuans* females from egg hatch to adult eclosion

Temperature (°C)	Development time (days)±SEM	Development rate (1/dev. time)
15	20.6±0.2	0.05
20	12.2±0.2	0.08
25	8.6±0.1	0.12
30	7.9±0.1	0.13
32	6.9±0.1	0.15
34	7.1[a]	0.14

[a] Only 1 female survived to adulthood at this temperature

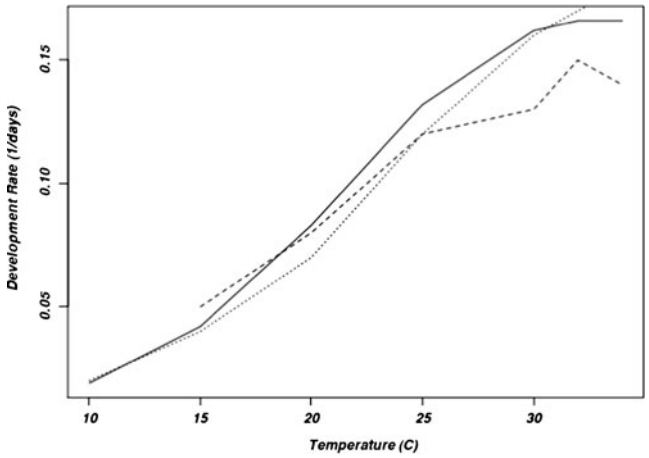

Fig. 4 Comparison of laboratory development rates for local strains of *Cx. pipiens* (*dotted line*) and *Cx. restuans* (*dashed line*) with model estimated rates (*solid line*)

T_{op} Optimal temperature for survival
S_{op} Survival rate at T_{op}
Var_{Sur} Variance of function

The approximate shape of the survival rate function relative to temperature resembled the Gaussian function. This is a common functional form for mosquito survival (e.g., Otero et al., 2006) and was supported qualitatively by field and laboratory trials, The same equation was used to estimate δ_I and δ_A (above); however, S_{op}, T_{op} and Var_{sur} for immature life stages and adults were different. The survival rate for immature cohorts was dependent on the average temperature over the cohort development period (egg laying to adult eclosion). In the models t represented 1 day. The boundaries for the rate parameterization were estimated by comparing the numbers of larvae that developed from the 1st to 4th instar larvae in the field study.

Moisture index

A moisture variable, M(t) was developed to take into account the cumulative impact of rainfall and evaporation on larval habitats. This index was created by summing the daily difference between precipitation, P, and evaporation, E, (mm) over the preceding 7 days.

$$M(t) = \sum_{D=t-6}^{t} P(D) - E(D) \quad (8)$$

Egg laying rate

Rainfall can have two principal impacts on mosquito population dynamics: (1) the increased near-surface humidity associated with rainfall may enhance mosquito flight activity and host-seeking behavior, and (2) rainfall can alter

the abundance and type of aquatic habitats available to the mosquito for deposition of eggs and the subsequent development of immature stages (Shaman and Day 2007).

The "Egg Laying Rate" function was dependent on the moisture index [(M), Fig. 5] and took a form similar to that of the survival rate. In principle, we assumed there was a positive correlation between egg laying rate and M.

$$\beta(t) = \mathrm{R_{Base\ egg}} + \frac{\mathrm{E_{max}}}{1 + \exp\left[-\frac{(\mathrm{M(t)} - \mathrm{E_{mean}})}{\mathrm{E_{var}}}\right]} \quad (9)$$

Where:

$E_{\max}$	Maximum egg laying rate above baseline
E_{mean}	Value at which the moisture index produces 50% of $E_{\max}$
E_{var}	Variance of function
$R_{\mathrm{Base\ egg}}$	Minimum constant fecundity rate

$R_{\mathrm{Base\ egg}}$ was included because we assumed that some oviposition activity occurred even when the moisture index was low (i.e., during periods with minimal or no rainfall). Our assumption of the egg laying rate value was based on laboratory observations within a reasonable range.

Diapause by photoperiod

Initially, the model did not include the influence of photoperiod and diapause. As a consequence, the simulated mosquito population always peaked at the end of the actual mosquito season. Based on work reported by Spielman (2001) with *Cx. pipiens* in the Northeast US, an estimate of the percent of diapausing adults was added as a function of decreasing hours of daylight (H_{D}).

$$\textit{Diapausing fraction} = -\mathrm{k}^{*}H_D(t) + b \quad (10)$$

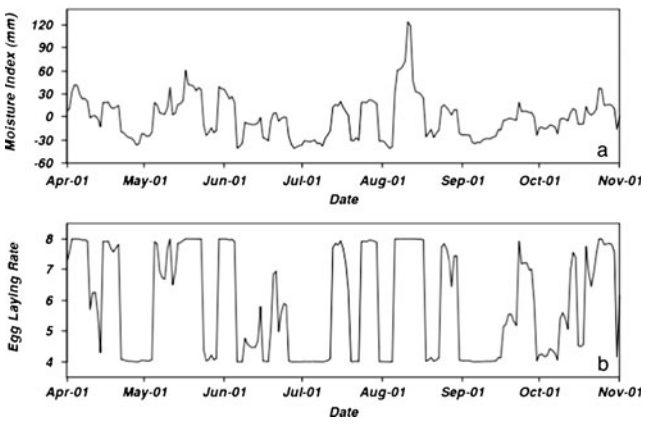

Fig. 5 Correspondence between **a** observed moisture index, and **b** calculated egg laying rate for a representative season

The effect of photoperiod started in mid-August when H_{D} dropped below 13 h. The parameter b was set at 15 times k to constrain the fraction at zero for 15 h daylight as shown by Spielman (2001).

Parameterization

Estimates of the function parameters were based on the most relevant information from the literature, and estimates of adult and immature survival from field and laboratory trials for New York strains of *Culex* species. However, under natural conditions, these values for the model survival, egg-laying and diapausing parameters might be suboptimal. Additionally, some parameters, such as egg laying rate as a function of moisture index, were impossible to determine experimentally. In order to obtain a more accurate model, the parameter space was explored to calibrate all functions with the exception of development rate, which was based solely on laboratory data (Table 3). This calibration was conducted by maximizing the correlation r between adult population from the model output and adult capture from traps using multiple years of data from the two sites.

Model simulations were run on the Earth and Atmospheric Sciences server at Cornell University (Linux AMD Opteron 64 bit). Using site-specific climatic data, the output of each run consisted of simulated adult mosquito population numbers over multiple years. For each run, a different set of parameter values were obtained by a scheduling algorithm where each parameter was scanned by intervals within the boundary. Table 3 presents the parameter and boundaries for both the development rate and degree day models. The highest correlation r and its associated parameters were recorded and retained during the simulation (Tables 3, 4).

Assessment of model performance

Capture data provide only relative measures of within-season mosquito population variation as indicated by Figs. 1 and 2. However, unequivocal data are not available. As a consequence, model performance was assessed based on the correlation r between adult population numbers from the model output and the adult capture from traps using multiple years of data. Wong et al. (2008) used a similar approach in conjunction with a genetic algorithm (GA) to obtain an objective fix on the position of tropical storm eyes. Correlation also formed the basis for tuning a GA to predict rainfall intensity (Tan et al. 2008). In both cases the GA was similar to the scheduling algorithm used here.

This approach was also necessary given the large differences in magnitude between trap counts and the total population simulated by the model. The difference in magnitude varied by site, with the simulation results as much as 50 times higher in magnitude than trap counts at

Table 3 Parameter space search estimates for parameters used in the model along with their upper and lower limits, and the best values. *DD* Degree day

Development rate model				DD model			
Parameter	Search boundary	Best value for site 1	Best value for site 2	Parameter	Search boundary	Best value for site 1	Best value for site 2
$R_{\text{Base egg}}$	0–5	4	2	$R_{\text{Base egg}}$	0–5	4	4
E_{max}	0–20	4	2	E_{max}	0–20	2	2
E_{mean}	-5 to 5	0	0	E_{mean}	−5 to 5	0	0
E_{var}	5 to 20	10	15	E_{var}	5 to 20	15	20
S_{op_Im}	0.6–0.95	0.95	0.95	S_{op_Im}	0.6–0.95	0.7	0.9
$Temp_{op\_Im}$	13–25	15	17	$Temp_{op\_Im}$	13–25	15	19
Var_{sur_Im}	5–20	5	5	Var_{sur_Im}	5–20	5	5
S_{op_Ad}	0.6–0.95	0.6	0.75	S_{op_Ad}	0.6–0.95	0.9	0.9
$Temp_{op\_Ad}$	13–25	17	23	$Temp_{op\_Ad}$	13–25	21	21
Var_{sur_Ad}	5-20	10	10	Var_{sur_Ad}	5–20	20	10
k	0.1–0.4	0.23	0.19	k	0.1–0.4	0.33	0.19
				S_{op_cohort}	0.08–0.3	0.12	0.08
				$Temp_{op\_cohort}$	13–25	15	19
				$Var_{sur\_corhort}$	5–20	5	10
For both models							
Initial adults	10	Minimum adults	1	Initial eggs	100	Minimum eggs	10

site 2 (Maryland) and 20 times higher at site 1 (New Jersey). Such discrepancies are not unexpected, Bell et al. (2005) found Mosquito Magnet traps captured up to 30 times more mosquitoes than did nearby NJ light traps. Similar between-trap differences were noted by Meeraus et al. (2008). Cooperband and Carde (2006) reported trapping efficiencies of less than 10% in wind tunnel experiments using a known number of released *Cx. quinquefasciatus*.

Table 4 Model performance for development rate model and DD models based on comparison of simulated abundance and observed trap capture

Development rate model								DD model							
Site 1				Site 2				Site 1				Site 2			
Year	r	Time between peaks (days)		Year	r	Time between peaks (days)		Year	r	Time between peaks (days)		Year	r	Time between peaks (days)	
		1st peak	2nd peak			1st peak	2nd peak			1st peak	2nd peak			1st peak	2nd peak
1990	0.5478	8	19	1975	0.6804	10	5	1990	0.1602	63	3	1975	0.6196	2	0
1991	0.7451	1	4	1977	0.5639	3	57	1991	0.6718	13	3	1977	0.7163	2	50
1992	0.7085	7	8	1982	0.6721	30 (5)[a]	30(5)	1992	0.3684	31 (5)	54 (28)	1982	0.1469	43 (5)	40(8)
1993	0.4280	13	11	1983	0.3966	0	75	1993	0.4014	19 (2)	25(4)	1983	0.5110	9	11
1997	0.6229	5	13	1984	0.7142	2	0	1997	0.6314	5	81	1984	0.7233	25 (1)	28(2)
1999	0.8474	3	4	1985	0.4509	5	12	1999	0.7590	21 (0)	23(2)	1985	0.3880	22	10
2001	0.8103	6	4					2001	0.7511	7	3				
Median	0.7085	6	8		0.6221	3(3)	21(9)		0.6314	19 (5)	23(3)		0.5653	16 (4)	20(9)

[a] If the 1 and 2nd peaks are switched, then the peak distance is shown parenthetically

In addition to the correlation between 7-day average capture and simulated abundance, model performance was also assessed based on the timing of peaks in the simulation and catch series. Peaks represent critical points of mosquito abundance, which may be associated with elevated disease transmission risk. Consequently, correspondence between the timing of observed and simulated peaks is an important measurement for determining the accuracy of the model and its potential for practical application. Prominent peaks above a threshold values were selected from the simulation series as described below (Eisenberg et al. 1995).

Definition of a peak

A peak appears at time t when:

$$\mathrm{N}(t-5)\ldots,\mathrm{N}(t-1)<\mathrm{N}(t)>\mathrm{N}(t+1)\ldots,\mathrm{N}(t+5) \quad (11)$$
$$\text{and } \mathrm{N}(t) > \text{Peak Threshold}$$

where $N(t)$ is the mosquito population at time t and the Peak Threshold is 70% of the maximum number of adults in the population over the entire season. An 11-day interval (5 days before and 5 days after t) was selected in order to identify the most prominent peaks over time. Shorter intervals failed to identify the occurrence of independent secondary peaks.

Timing of the two highest peaks

Over each year, the timing of the 1st and 2nd highest peaks in the adult simulation and capture series were compared (Table 4). Secondary peaks that were too close to the primary peak were not considered. The distance for excluding such peaks was set at both 10 and 20 days. These criteria assured that the 2nd highest peak was separated from the primary peak by at least 10 or 20 days.

Model simulation

To check the reliability of the model, two different approaches were used. First, a 6-year subset of data from site 1 was selected to conduct the parameter space search. After obtaining the best model, the adult mosquito population was simulated for the year that was excluded from the subset and compared it to the actual trap data (Table 5). In the second approach the best model from site 1 parameterized over all 7 years was applied to simulate mosquito capture during a different year at an independent location (Freeville Farm, NY).

Results

Model performance

Table 4 presents correlation coefficients and differences in the timing of peaks between the simulations and mosquito trap data. These comparisons were made for both the development rate and DD models for both sites. In general, the basic patterns of seasonal abundance and mosquito population peaks were correctly simulated, as was the timing of commencement and last appearance of mosquitoes based on the first and last captures. Details of the performance for each model type are presented below. Optimal values for each parameter are presented in Table 3.

Development rate model

New Jersey (Site 1)

The best model for site 1 simulates adult populations with average r values of 0.6728 over 7 years (Fig. 6a), where r is the correlation between adult population numbers from model simulation and actual adult capture data from surveillance traps (Table 4). Correlation of this magnitude agrees well with the between-trap correlation for sites in Middlesex County.

This model also simulated population peaks within 5 days (Table 4). Simulated population peaks for this site were well matched with the actual trap data in both timing and relative amplitude (except for 1991) (Fig. 6a). The years with the highest simulated abundance (1990, 1992, 2001) matched the years in which capture was the highest. Similarly, lower capture in 1993 and 1997 was reflected by lower simulated abundance. Despite relatively high capture in 1991 compared to the other years, the simulated

Table 5 Results of correlation between simulated population in year n and capture based on a 6-year simulation with year n excluded for site 1

Omitted year	1990	1991	1992	1993	1997	1999	2001
r fitted years[a]	0.6960	0.6628	0.6679	0.7136	0.6812	0.6462	0.6524
r omitted years[b]	0.5366	0.7512	0.7041	0.4356	0.6457	0.8245	0.8038

[a] Average correlation between simulated abundance and capture over the six years used to develop the model

[b] Correlation between simulated abundance and capture in the year excluded in model development

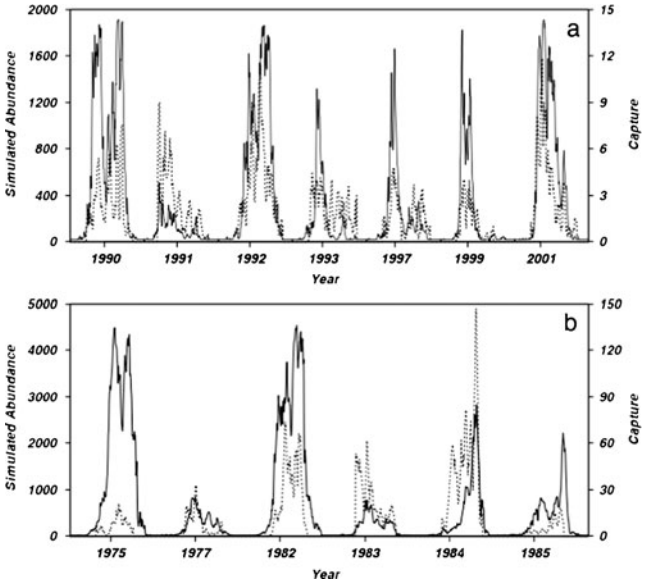

Fig. 6 Comparison of simulated mosquito abundance (*solid line*) and capture (*dotted line*) at **a** North Brunswick, NJ (Site 1), and **b** near Cambridge Maryland (Site 2) based on the development rate model

abundance in that year was the lowest. Perhaps due to the low moisture index, the 1991data did not accurately represent the true availability of mosquito breeding sites.

Maryland (Site 2)

The correlation of the site 2 model with the capture data was lower (Fig. 6b) than site 1. The average *r* value was 0.5797, which again is typical of the correlation in capture from separate nearby traps.

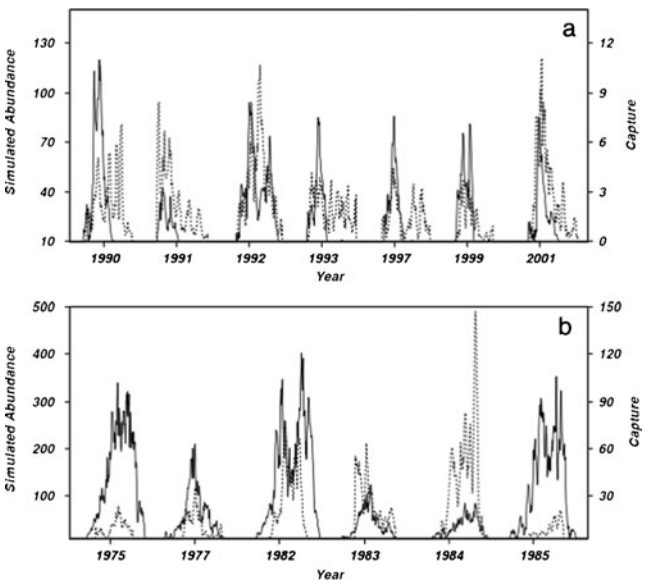

Fig. 7 Comparison of simulated mosquito abundance (*solid line*) and capture (*dotted line*) at **a** North Brunswick, NJ (Site 1), and **b** near Cambridge Maryland (Site 2) based on the DD model

The timing of simulated population peaks matched the trap data well, but was not as close a match as for site 1. There was also generally good agreement in the year-to-year variations in relative abundance and the first and last seasonal appearances of adults. Relatively low capture in 1977, 1983 and 1985 was reflected by low simulated abundance. Higher capture in 1982 and 1984 also corresponded with relatively high simulations. However, the high simulated abundance in 1977 was associated with relatively low capture.

Degree day model

New Jersey (Site 1)

The DD model for Site 1 did not perform as well as the development rate model (Fig. 7a). The average correlation (*r*) for this model was 0.5347, still in line with the between-trap values for observed data (Table 4). Unlike with the development rate model, with the DD model, simulated peaks early in the season matched the timing of peaks in the trap data well, but late peaks did not match (Fig. 7a). The DD model simulations also did not reflect the observed year-to-year variations in capture, or the start and, particularly, the end of seasonal mosquito collections as well as did the development rate model.

Maryland (Site 2)

As with site 1, the development rate model for site 2 showed a better correlation with the trap data than the DD model (r=0.5175). This model tended to simulate population peaks weeks earlier than actual capture data (Table 4)

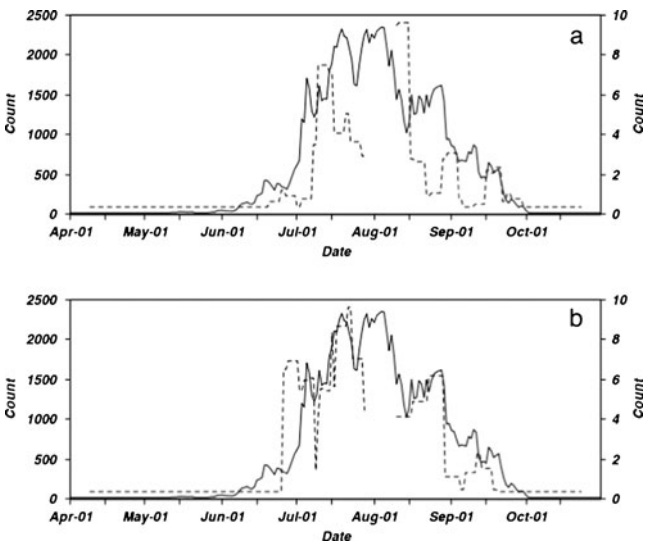

Fig. 8 Comparison of development model simulation (*dotted line*) and capture (*solid line*) for **a** CDC trap, and **b** NJ trap capture at Freeville, NY during 2006

and did not provide a good simulation of the interannual variations in capture, or the start and end of adult mosquito activity (Fig. 7b).

Independent validation

Results for the development rate model at site 1 using the approach where each year was dropped from model optimization and subsequently simulated are presented in Table 5. A high correlation between the trap data and simulated year was obtained using this approach, but the strength of this correlation varied depending on which year was dropped from optimization. Nonetheless, the correlation between the simulations and capture was of a similar magnitude to that of capture at sites within the county.

In the second approach, the model for site 1 was applied to simulate mosquito abundance at the independent Freeville, NY site. Local weather data collected at the site were used in the model. Co-located CDC trap and NJ trap data were compared with the simulated adult populations. The capture data were smoothed by averaging over 7 days to match the averaging used in the simulations. The model predicted population dynamics well, with correlations comparable to the development sites (r=0.70 for simulated versus maximum capture from the CDC and NJ traps) and reasonable timing of peaks (Fig. 8). Figure 2 highlights the difficulties associated with the available trap data, as the day-to-day correlation between the two co-located traps was low during many periods.

Discussion

Two different models to simulate *Culex* mosquito vector populations in the northeastern US were developed. The models focused on the development of Northeast strains of *Cx. pipiens* and *Cx. restuans* mosquitoes. Model parameters were optimized using long-term data sets from locations in the northeastern US. These models perform well in simulating the timing of *Culex* mosquito populations and the pattern of within-season mosquito abundance as indicated by capture data. However, the model simulations of abundance consistently exceed the capture counts. This is not unexpected given limited trap capture efficiencies. Correlation between simulated abundance and capture, however, agreed with that of capture between traps located across a county-size area (e.g., traps separated by tens of kilometers). The nuances of site-specific meteorological and environmental conditions make it difficult to simulate abundance at the microhabitat level. However, at a larger spatial scale that is better represented by available operational meteorological data, key components of the annual cycle of mosquito abundance such as early summer onset, fall decline and within season abundance peaks and lulls are simulated by the model.

These models differ from existing models based on the inclusion of variables such as the moisture index, which takes into account the effect of water deficit, precipitation and evaporation on mosquito populations. A function to express egg production included a baseline egg production rate that could be adjusted upward in response to an increase in the moisture index. The addition of this function, especially with the baseline egg production rate, improved earlier versions of model significantly, as did the inclusion of a function for the impact of diapause. Unlike most published models, which are based on relatively short (e.g., 3-year) development samples (Ahumada et al. 2004; Shone et al. 2006), up to 7 years of data were used to tune the model parameters developed in this study.

Assessment of development rate and DD models indicated that the development rate model performed better. When applied to simulate mosquito populations at a new site in 2006, the development rate model obtained high predictive power. Better results were obtained when simulating the beginning of the mosquito season and overall correlation with capture using the development time estimates from laboratory studies of local geographic stains of *Cx. restuans* rather than the average time from both *Cx. pipiens* and *Cx. restuans*. This was most likely due to greater early season abundance of *Cx. restuans* in the Northeast than *Cx. pipiens*. This difference in activity highlights the importance of optimizing model parameters for relevant mosquito species and geographic strains. Unfortunately this was not possible given the constraint that these two species were grouped in the available long-term capture.

In the New York and New Jersey sites, *Cx. pipiens* and *Cx. restuans* are the predominant *Culex* species. Two other species, *Cx. territans* and *Cx. salinarius*, are present, but rarely collected, in NJ traps or CDC traps in the region. In Maryland, *Cx. pipiens* and *Cx. salinarius* were the dominant species in the collection data. This led to problems with application of the model to the more southerly location.

Although the DD model was expected to be more adaptable to other regions than the development rate model, it did not perform as well. This was especially apparent when applying the model developed for one site (for example, site 1) to another site (such as site 2). This lack of good correlation may have been due to geographic differences in temperature-dependent development of local vector species. In addition, the presence of *Cx. salinarius* at the Maryland site may have contributed to the lack of fit with this data. *Cx. salinarius* is present, but rare, in our collections from Central New York. In addition, there can be significant bias and variation in the composition of

mosquito collections based on the type of trap and spatial location of traps within different habitats (Brown et al. 2008).

The development rate model for predicting adult *Culex* mosquito populations in the Northeast US is robust. It was capable of simulating population trends in terms of the timing of abundance peaks and the weekly variations of capture data in each of 7 years characterized by different climatological conditions. The model was also able to simulate the relative year-to-year variations in the capture data. It was difficult to directly compare simulated abundance with the actual population, as the relationship between the available capture data and total abundance is complex and not readily obtainable.

Further development of this model will include incorporation of vector-borne pathogen parameters for estimating risk and the development of user-friendly interfaces for local scale adaptation. In addition, this model may be useful for conceptually understanding the relative impact that climate change may have on mosquito habitats and the need for scaling data from regional areas to the level of mosquito microhabitats.

Acknowledgments Support for this research was provided by grants from Hatch (NYC-139410) and the National Oceanic and Atmospheric Administration (NA04OAAR4310184). Rod Schmidt, Tony Aquaviva and Gregory Glass generously provided long-term adult mosquito data.

References

Ahumada JA, Lapointe D, Samuel MD (2004) Modeling the population dynamics of *Culex quinquefasciatus* (Diptera: Culicidae), along an elevational gradient in Hawaii. J Med Entomol 41:1157–1170

Andreadis T, Thomas MC, Shepard J (2005) Identification guide to the mosquitoes of Connecticut. Conn. Agric Exp Stn 966:1–173

Bell JA, Mickelson NJ, Vaughan JA (2005) West nile virus in host-seeking mosquitoes within a residential neighborhood in Grand Forks, North Dakota. Vector-borne Zoonot 5:373–382

Brown HE, Paladini M, Cook RA, Kline D, Barnard D, Fish D (2008) Effectiveness of mosquito traps in measuring species abundance and composition. J Med Entomol 45:517–521

CDC (1999a) From the centers for disease control and prevention. Update: West Nile-like viral encephalitis—New York, 1999. JAMA 282:1714

CDC (1999b) Outbreak of west Nile-like viral encephalitis—New York. Morb Mortal Wkly Rep 48:845–849

Cooperband MF, Carde RT (2006) Orientation of *Culex* mosquitoes to carbon dioxide baited traps: flight manoeuvres and trapping efficiency. Med Vet Entomol 20:11–26

DeGaetano AT (2005) Meteorological effects on adult mosquito (*Culex*) populations in metropolitan New Jersey. Int J Biometeorol 49:345–353

Derouich M, Boutayeb A, Twizell EH (2003) A model of dengue fever. Biomed Eng Online 2:4

Ebi KL, Mills DM, Smith JB, Grambsch A (2006) Climate change and human health impacts in the United States: an update on the results of the US national assessment. Environ Health Perspect 114:1318–1324

Eisenberg JN, Reisen WK, Spear RC (1995) Dynamic model comparing the bionomics of two isolated *Culex tarsalis* (Diptera: Culicidae) populations: model development. J Med Entomol 32:83–97

Esteva L, Vargas C (1999) A model for dengue disease with variable human population. J Math Biol 38:220–240

Focks DA, Haile DG, Daniels E, Mount GA (1993a) Dynamic life table model of a container-inhabiting mosquito, *Aedes aegypti* (L.) (Diptera: Culicidae). Analysis of the literature and model development. J Med Entomol 30:1003–1017

Focks DA, Haile DG, Daniels E, Mount GA (1993b) Dynamic life table model of a container-inhabiting mosquito, *Aedes aegypti* (L.) (Diptera: Culicidae). Simulation results and validation. J Med Entomol 30:1018–1028

Focks DA, Daniels E, Haile DG, Keesling JE (1995) A simulation model of the epidemiology of urban dengue fever: literature analysis, model development, preliminary validation, and samples of simulation results. Am J Trop Med Hyg 53:489–506

Gerade BB, Lee SH, Scott TW, Edman JD, Harrington LC, Kitthawee S, Jones JW, Clark JM (2004) Field validation of *Aedes aegypti* (Diptera: Culicidae) age estimation by analysis of cuticular hydrocarbons. J Med Entomol 41:231–238

Harrington LC, Poulson RL (2008) Considerations for accurate identification of adult *Culex restuans* (Diptera: Culicidae) in field studies. J Med Entomol 45:1–8

Koenraadt CJ, Harrington LC (2008) Flushing effect of rain on container-inhabiting mosquitoes *Aedes aegypti* and *Culex pipiens* (Diptera: Culicidae). J Med Entomol 45:28–35

Krockel U, Rose A, Eiras AE, Geier M (2006) New tools for surveillance of adult yellow fever mosquitoes: comparison of trap catches with human landing rates in an urban environment. J Am Mosq Contr 22:229–238

Kunkel KE, Novak RJ, Lampman RL, Gu W (2006) Modeling the impact of variable climatic factors on the crossover of *Culex restuans* and *Culex pipiens* (Diptera: culicidae), vectors of west nile virus in Illinois. Am J Trop Med Hyg 74:168–173

Means RG (1987) Mosquitoes of New York: Part II. Genera of Culicidae other than Aedes occurring in New York, State Education Department, Albany, NY

Meeraus WH, Armistead JS, Arias JR (2008) Field comparison of novel and goldstandard traps for collecting *Aedes albopictus* in northern Virginia. J Am Mosq Contr 24(2):244–248

Ngwa G (2004) Modelling the dynamics of endemic malaria in growing populations. Dis Cont Dyn Syst Ser B 4:1173–1202

Otero M, Solaril HG, Schweigmann N (2006) Stochastic population dynamics model for *Aedes Aegypti*: formulation and application to a city with temperate climate. B Math Biol 68:1945–1974

Reisen WK, Boyce K, Cummings RC, Delgado O, Gutierrez A, Meyer PR, Scott TW (1999) Comparative effectiveness of three adult mosquito sampling methods in habitats representative of four different biomes of California. J Am Mosq Contr 15:24–31

Rueda LM, Patel KJ, Axtell RC, Stinner RE (1990) Temperature-dependent development and survival rates of *Culex quinquefasciatus* and *Aedes aegypti* (Diptera: Culicidae). J Med Entomol 27:892–898

Shaman J, Day JF (2007) Reproductive phase locking of mosquito populations in response to rainfall frequency. PLoS ONE 2:e331

Shone SM, Curriero FC, Lesser CR, Glass GE (2006) Characterizing population dynamics of *Aedes sollicitans* (Diptera: Culicidae) using meteorological data. J Med Entomol 43:393–402

Spielman A (2001) Structure and seasonality of nearctic *Culex pipiens* populations. Ann NY Acad Sci 951:220–234

Tan TZ, Lee GKK, Liong SY, Lim TK, Chu J, Hung T (2008) Rainfall intensity prediction by a spatial-temporal ensemble. Neural Networks. 2008 International Joint Conference on

Neural Networks (IJCNN 2008), IEEE World Congress on Computational Intelligence, http://ieeexplore.ieee.org/stamp/stamp.jsp?arnumber=4634030&isnumber=4633757

Wagner TL, Olson RL, Willer JL (1991) Modeling arthropod development time. J Agr Entomol 8:251–270

Walraven R (1978) Calculating the position of the sun. Sol Energy 20:393–397

White DJ (2006) West Nile virus: detection, surveillance, and control. Ann NY Acad Sci 951:74–83

Wong KY, Yip CL, Li PW (2008) Automatic tropical cyclone eye fix using genetic algorithm. Exp Sys Appl 34:643–656

Wonham MJ, De-Camino-Beck T, Lewis MA (2004) An epidemiological model for West Nile virus: invasion analysis and control applications. Proc Roy Entomol Soc B 271:501–507